

## Quantized current in a quantum dot turnstile

L.P. Kouwenhoven, A.T. Johnson, N.C. van der Vaart, D.J. Maas, C.J.P.M. Harmans

*Faculty of Applied Physics, Delft University of Technology, P.O. Box 5046, 2600 GA Delft, Netherlands*

and

C.T. Foxon

*Philips Research Laboratories, Redhill, Surrey RH1 5HA, UK*

Received 1 June 1991; accepted for publication 26 August 1991

We have observed a quantized current in a lateral quantum dot defined by metal gates in the two-dimensional electron gas (2DEG) of a GaAs/AlGaAs heterostructure. By modulating the tunnel barriers in the 2DEG with two phase shifted RF signals, and employing the Coulomb blockade of electron tunneling, we produced quantized current plateaus in the current–voltage characteristics at integer multiples of  $ef$ , where  $f$  is the RF frequency. This demonstrates that an integer number of electrons pass through the quantum dot each RF cycle.

The ability to control electronic current on a single-electron level has become feasible by employing the Coulomb blockade in submicron devices. This single-electron control is not only interesting from a fundamental point of view, but also for obtaining a current standard and possibly for various device applications [1]. RF studies in conjunction with Coulomb effects have been performed by Geerligs et al. [2], who applied a RF signal to the central island of a sample of four metal tunnel junctions in series. They observed a plateau at a current  $I = ef$ , with  $f$  the frequency of the RF signal, demonstrating that exactly one electron per RF cycle passed through their so-called *turnstile* device. Here we present the realization of a turnstile operation in a semiconductor quantum dot defined by metal gates in a two-dimensional electron gas (2DEG) [3]. In contrast to the metal systems, our quantum dot turnstile relies on the ability to induce *oscillating tunnel barriers* between the quantum dot and the wide 2DEG regions by applying RF signals to the gates. The inset of fig. 3 is a SEM photograph of the gate geometry, which is fabricated on top of a GaAs/AlGaAs heterostructure containing a

2DEG about 100 nm below the surface. The ungated 2DEG has a mobility of  $2.3 \times 10^6$   $\text{cm}^2/\text{V} \cdot \text{s}$  and an electron density of  $1.9 \times 10^{15}$   $\text{m}^{-2}$  at 4.2 K. We denote gate F as the finger gate, gates 1 to 4 as quantum point contact (QPC) gates, and gate C as the center gate. We do not use QPC gates 3 and 4; these gates are grounded and have no effect on the 2DEG. Applying  $-400$  mV to gates F, C, 1, and 2 depletes the electron gas underneath them and forms a quantum dot with a diameter of about  $0.8 \mu\text{m}$  in the 2DEG. The narrow channels between gates 1–C, and 2–C are pinched-off at this gate voltage. Electron transport occurs only through the constrictions induced by gates 1–F, and 2–F, which couple the dot to the two wide 2DEG regions.

Charging effects become important when the gate voltages are such that the constrictions form tunnel barriers with conductances  $G_1, G_2 \ll 2e^2/h$ . On varying the voltage on the center gate, the conductance  $G$  of the dot is expected to oscillate between zero (Coulomb blockade) and non-zero (no Coulomb blockade). These *Coulomb oscillations* have recently been observed in quantum dots [4,5] and are shown in the upper inset of

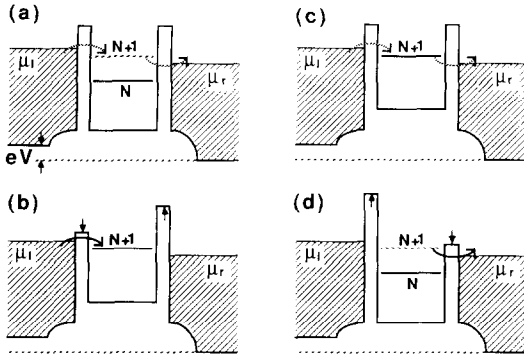


Fig. 1. Potential landscape through the quantum dot.  $\mu_l$  and  $\mu_r$  are the electrochemical potentials of the left and right reservoirs, and  $V = (\mu_l - \mu_r)/e$  is the bias voltage. The level  $N$  indicates  $\mu_d(N)$  when  $N$  electrons are confined in the quantum dot, while the level  $(N + 1)$  indicates  $\mu_d(N + 1)$ . (a) to (d) are four stages of a RF cycle where the probability for electron tunneling is large when the barrier is low (solid arrows), and small when the barrier is high (dashed arrows).

fig. 2 for our sample. All measurements are performed at 10 mK and zero magnetic field. The period of the oscillations is 4.6 mV; *each period corresponding to a change of one electron in the dot*. For unequal tunnel barriers, a stepwise increase of the current  $I$  upon increasing the bias voltage  $V$  is expected [1]. This *Coulomb staircase* is shown in the lower inset of fig. 2. The five different curves correspond to different center gate voltages: the lowest curve is at a Coulomb oscillation minimum, the curve in the middle at a conductance peak, and the uppermost curve at the next minimum. The width  $\Delta V = 0.67$  mV of the current plateaus is a direct measure of the charging energy;  $e\Delta V = e^2/C$ , from which we deduce the total capacitance  $C = 2.4 \times 10^{-16}$  F.

We now demonstrate that with oscillating tunnel barriers, the Coulomb oscillations and staircase are determined by the frequency of the applied RF signals. Fig. 1 represents four stages of a RF cycle, where the tunnel barriers oscillate with a phase difference of  $\pi$  [6]. In (a) the dashed arrows indicate possible tunneling via the  $\mu_d(N + 1)$  charge state.  $\mu_d(N)$  is the electrochemical potential when  $N$  electrons are confined in the dot. Addition of an extra electron to the dot increases the electrochemical potential by  $\mu_d(N + 1) - \mu_d(N) = e^2/C$ . When the left barrier is reduced, the probability for the  $(N + 1)$  electron

to tunnel into the dot is strongly enhanced, as illustrated by the solid arrow in (b). Simultaneously, the increase of the right barrier makes the probability to tunnel out of the dot virtually zero. Tunneling into the dot of a second electron is prevented by the Coulomb blockade. At half the cycle time, shown in (c), the barriers are in their equilibrium position again, but compared with (a), one extra electron is confined in the dot. The  $(N + 1)$  electron tunnels out when the right barrier is reduced, and simultaneously, the left barrier is increased, which is illustrated in (d). Completing the cycle, yields the initial situation shown in (a), and exactly one electron has passed through the quantum dot. Repeating this process with a frequency  $f$  results in a current  $I = ef$ . Increasing the bias voltage, thereby increasing the number  $n$  of charge states contained in the energy interval between  $\mu_l$  and  $\mu_r$ , produces a quantized current  $I = nef$ , corresponding to frequency determined current steps in the Coulomb staircase. The steps in the staircase come at voltage intervals of  $e/C$ , from which we expect an average conductance  $\langle G \rangle = ef/(e/C) = fC$ . An estimate of the accuracy of this quantized current for our experimental values [3] gives about 0.1%, somewhat better than observed in the data below.

In fig. 2 we show measured  $I-V$  characteristics

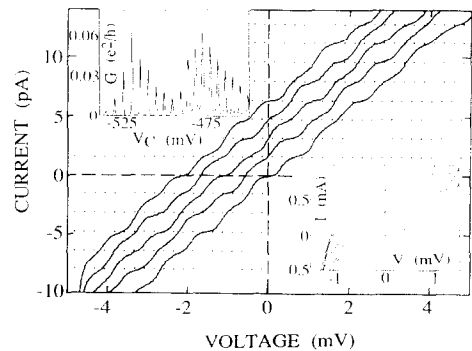


Fig. 2. Main figure:  $I-V$  characteristics when two phase shifted RF signals are applied with a frequency  $f = 10$  MHz, showing current plateaus at integer multiples of  $ef$  (dotted lines). The curves correspond to different center gate voltages and are offset for clarity by an integer times  $ef$ . Upper inset: Coulomb conductance oscillations versus center gate voltage. Lower inset: Coulomb staircase in the  $I-V$  characteristics (the curves correspond to different center gate voltages and are offset for clarity).

with 10 MHz RF signals with a phase difference of  $\pi$  applied to QPC gates 1 and 2. The quantized current values  $nef$  are indicated by dotted lines [ $e(10 \text{ MHz}) = 1.6 \text{ pA}$ ]. The curves correspond to different center gate voltages, and are offset from each other by  $ef$ . Fig. 2 shows that on applying RF, the  $I$ - $V$  curves have current plateaus at integer multiples of  $ef$ , demonstrating that a discrete number of electrons pass through the quantum dot each RF cycle. Some of the plateaus are missing or weakly developed. This plateau averaging occurs for roughly equal tunnel barriers: the bias voltage drops across both barriers instead of dropping mainly over one barrier, as required for a well-developed staircase [1].

The current plateaus are illustrated in fig. 3, where for  $f = 10 \text{ MHz}$  the same curves are shown as in fig. 2, but now without offsets. The dotted lines indicate the quantized current values  $nef$

for  $f = 10 \text{ MHz}$ . As expected from the model, the curves have crossings that occur at current multiples of  $ef$  and voltage multiples of  $e/C$ , for  $n$  between  $-7$  and  $7$ . To demonstrate scaling with frequency, also  $I$ - $V$  curves are shown for  $f = 5$  and  $20 \text{ MHz}$ , which have respectively, twice and half as many crossings as the curves for  $10 \text{ MHz}$ . Moreover, the average conductance  $\langle G \rangle = fC$  scales with frequency, and is in agreement with the value for  $C$  obtained from the Coulomb staircase shown in the lower inset of fig. 2. An alternative way of measuring the same curves [2] is shown in the lower inset of fig. 3, where the current is shown versus center gate voltage for different bias voltages and  $f = 10 \text{ MHz}$ . The current is independent of center gate voltage and equal to  $nef$  when the bias voltage corresponds to a crossing in the  $I$ - $V$  curves. In between, the current oscillates with a period equal to that of

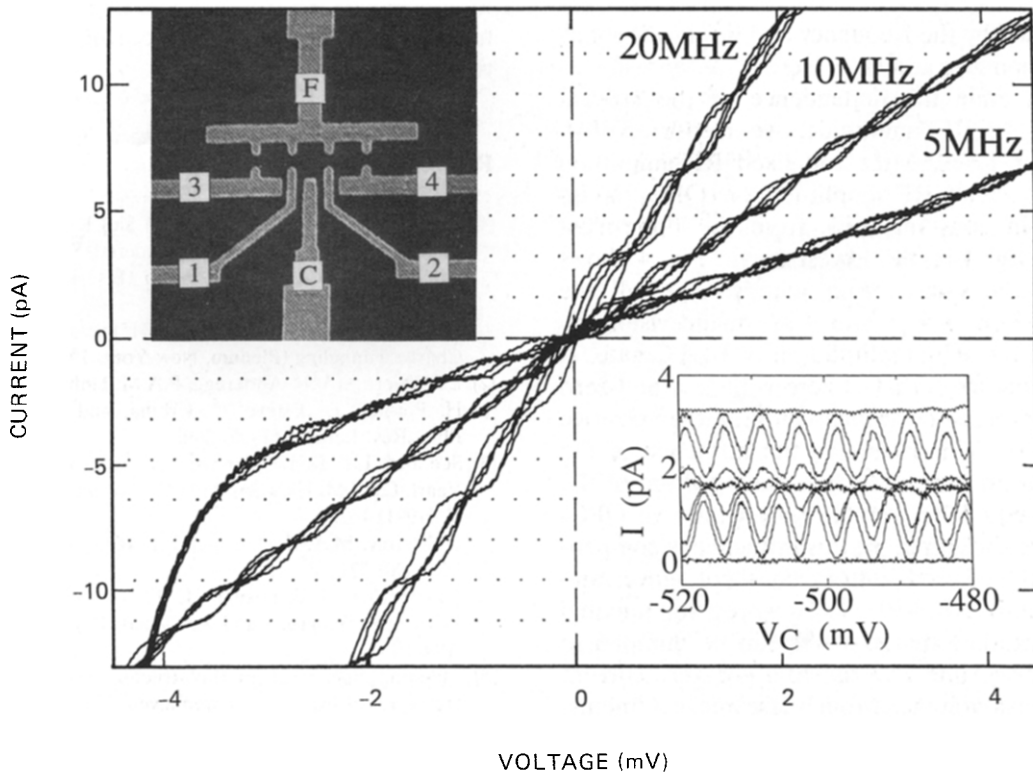


Fig. 3. Main figure:  $I$ - $V$  curves for RF frequency  $f = 5, 10,$  and  $20 \text{ MHz}$ , demonstrating scaling with frequency. Dotted lines indicate multiples of  $ef$  for  $f = 10 \text{ MHz}$ . Upper inset: Gate geometry. Lower inset: Current versus center gate voltage for  $f = 10 \text{ MHz}$  and different fixed bias voltages. The current oscillations have a frequency determined amplitude in the interval between  $nef$  and  $(n + 1)ef$ .

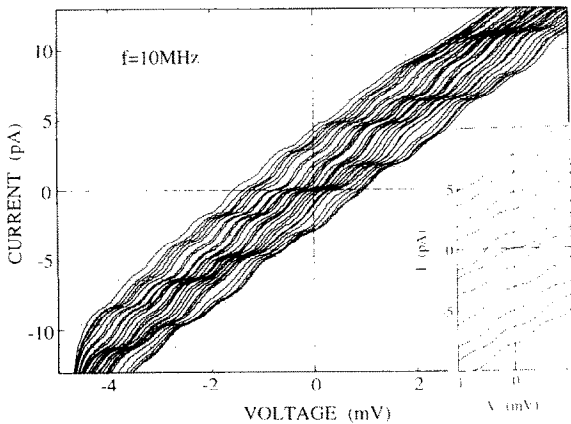


Fig. 4.  $I$ - $V$  characteristics with fixed RF amplitude on QPC<sub>2</sub> and different RF amplitudes on QPC<sub>1</sub>, showing all the current plateaus from  $-7ef$  to  $7ef$ . Inset:  $I$ - $V$  characteristics with current plateaus from  $-5ef$  to  $5ef$  at zero bias voltage, demonstrating discrete electron pumping.

the Coulomb oscillations shown in the upper inset of fig. 2. However, the amplitude is now determined by the frequency and lies in the interval between  $nef$  and  $(n + 1)ef$ .

To examine the dependence of the current plateaus on RF amplitude, we measured  $I$ - $V$  curves for  $f = 10$  MHz and fixed RF amplitude on QPC<sub>2</sub>. The RF amplitude on QPC<sub>1</sub> is increased in constant steps from the uppermost curve in fig. 4 to the lowest curve. Fig. 4 shows that for the same center gate voltage, all the plateaus from  $n = -7$  to  $7$  are made visible by changing the RF amplitude on one QPC gate. A striking feature is that at zero voltage a non-zero current is observed, which can be either positive or negative. This is due to the influence of the RF signal on the conduction band bottom of the dot. For equal RF amplitudes on the two QPCs and phase difference  $\pi$ , this influence is compensated, so the band bottom does not move, and consequently  $I(V = 0) = 0$ . However, for unequal RF amplitudes, charge states can be pumped to higher energy and give rise to a non-zero current at zero bias voltage. From these measurements, we have been able to deduce the effect on the quantized current plateaus of the center gate voltage, the RF amplitudes, and the phase difference. To demonstrate the tunability of the quan-

tum dot turnstile, we have measured the pumping in more detail, which is shown in the inset of fig. 4. Tuning the different parameters, we found quantized current plateaus from  $n = -5$  to  $5$  around zero voltage, showing that a discrete number of electrons are pumped per RF cycle.

In summary, we have realized a quantum dot turnstile using oscillating tunnel barriers. The observation of quantized current plateaus at multiples of  $ef$  demonstrates the ability to control current on a single-electron level.

We wish to thank L.J. Geerligs, K.K. Likharev, J.E. Mooij, and B.J. van Wees for stimulating discussions, A. van der Eenden for his contributions to the device fabrication, and the Delft Institute for MicroElectronics and Submicron-technology for the use of their facilities. Financial support from FOM and ESPRIT (project 3133, NANSDEV) is gratefully acknowledged. L.P.K. acknowledges the Sakaki Quantum Wave Project in Tokyo for the hospitality during the preparation of the manuscript.

## References

- [1] See for two reviews: D.V. Averin and K.K. Likharev, in: Quantum Effects in Small Disordered Systems, Eds. B. Altshuler, P. Lee and R. Webb (Elsevier, Amsterdam, 1990); H. Grabert, J.M. Martinis and M.H. Devoret, Eds., Single Charge Tunneling (Plenum, New York, 1991).
- [2] L.J. Geerligs, V.F. Andereg, P.A.M. Holweg, J.E. Mooij, H. Pothier, D. Esteve, C. Urbina, and M.H. Devoret, Phys. Rev. Lett. 64 (1990) 2691.
- [3] See also: L.P. Kouwenhoven, A.T. Johnson, N.C. van der Vaart, C.J.P.M. Harmans and C.T. Foxon, Phys. Rev. Lett. 67 (1991) 1626.
- [4] U. Meirav, M.A. Kastner and S.J. Wind, Phys. Rev. Lett. 65 (1990) 771; P.L. McEuen, E.B. Foxman, U. Meirav, M.A. Kastner, Y. Meir, N.S. Wingreen and S.J. Wind, Phys. Rev. Lett. 66 (1991) 1926.
- [5] Charging experiments on this structure without RF signals are reported by: L.P. Kouwenhoven, N.C. van der Vaart, A.T. Johnson, C.J.P.M. Harmans, J.G. Williamson, A.A.M. Staring and C.T. Foxon, Festkörperprobleme/Advances in Solid State Physics, Vol. 31, Ed. U. Rössler (Vieweg, Braunschweig, 1991) p. 329.
- [6] A.A. Odintsov, Appl. Phys. Lett. 58 (1991) 2695.